

Abatement efficiency and fate of EPA-Listed PAHs in aqueous medium under simulated solar and UV-C irradiations, and combined process with TiO₂ and H₂O₂

Navid Kargar^{1*} • Ali Reza Amani-Ghadim² • Amir Abbas Matin³ • Golnar Matin⁴ • Hasan Baha Buyukisik⁵

¹ Department of Marine-Inland Water Sciences and Technology, Faculty of Fisheries, Ege University, 35100 Bornova, Izmir, Turkey

² Department of Chemistry, Faculty of Sciences, Azarbaijan Shahid Madani University, 53714-161 Tabriz, Iran

³ Department of Chemistry, Faculty of Sciences, Azarbaijan Shahid Madani University, 53714-161 Tabriz, Iran

⁴ Department of Marine-Inland Water Sciences and Technology, Faculty of Fisheries, Ege University, 35100 Bornova, Izmir, Turkey

⁵ Department of Marine-Inland Water Sciences and Technology, Faculty of Fisheries, Ege University, 35100 Bornova, Izmir, Turkey

 <http://orcid.org/0000-0002-6939-0284>

 <http://orcid.org/0000-0003-3279-5170>

 <http://orcid.org/0000-0001-8264-8414>

 <http://orcid.org/0000-0002-1286-8611>

 <http://orcid.org/0000-0002-5855-4300>

*Corresponding author: navidkargar@gmail.com

Received date: 09.04.2019

Accepted date: 05.09.2019

How to cite this paper:

Kargar, N., Amani-Ghadim, A.R., Matin, A.A., Matin, G. & Buyukisik, H.B. (2020). Abatement efficiency and fate of EPA-Listed PAHs in aqueous medium under simulated solar and UV-C irradiations, and combined process with TiO₂ and H₂O₂. *Ege Journal of Fisheries and Aquatic Sciences*, 37(1), 15-27. DOI: 10.12714/egejfas.37.1.03

Abstract: Photolytic degradation of dissolved compounds of 16 EPA-Listed PAHs in aqueous medium, exposed to ultraviolet/ titanium dioxide (UV-C/TiO₂), xenon light/ titanium dioxide (Xe/TiO₂), xenon light/ hydrogen peroxide (Xe/H₂O₂) and ultraviolet/ hydrogen peroxide (UV-C/H₂O₂) was studied. The compounds which detected above detection limit of applied analytical method and instrument include: naphthalene (Nap), acenaphthylene (Acy), acenaphthene (Ace), fluorene (Flu), fluoranthene (Flu) and pyrene (Pyr) survived. A time-course experiment (0, 1, 2, 5, 12 min) was performed to determine the fate of PAHs profile along treatments. After accomplishment of the removal process \sum_6 PAHs ranked as follow: UV-C/TiO₂ > Xe/TiO₂ > UV-C > Xe > Xe/H₂O₂, and UV-C /H₂O₂ with estimated values of 76.38, 23.02, 22.55, 2.78, 0.00 and 0.00% of the concentration values at the beginning of the treatment, respectively. High efficiency of Xe/H₂O₂ treatment process (100.00%) at the end of treatment and the structure of residual PAHs which changed to the lighter compounds (2,3-ringed PAHs) before accomplishment of the removal process were proven. Generally, low resistance of Flu to all treatment conditions was observed. Total removal of Nap was considered to be a characteristic PAH compound for completion of the removal of PAHs. Mutate of parent PAH compounds and intermediates were analyzed by gas chromatography-mass spectrometry (GC-MS) and the results suggest the evaluating the toxicity of the treated water due to by-product formation concerns.

Keywords: Water treatment, advanced oxidation processes (AOPs), photodegradation, endocrine disrupting chemicals (EDCs), 16 EPA-Listed PAHs

INTRODUCTION

Owing to different varieties of human activities, numerous organic and inorganic chemicals are constantly discharged into different component of the environment. Organic pollutants represent widely used ubiquitous substances, also they can be found as by-products through natural and/or human-induced processes. Polycyclic aromatic hydrocarbons (PAHs) (CASRN: 130498-29-2) consist of two or more fused aromatic rings and constitute an important group of environmentally persistent and toxic organic pollutants. Incomplete organic combustion is the main source of PAHs while introduction of PAHs into the environment is a consequence of both natural events (e.g., volcanic activities, forest fires, and natural leakage of natural gas and crude oil) and human activities (e.g., burning of fossil fuels, extraction, transportation, and refining operations of fossil fuels, waste incineration, and smoking) (Fechner, 2015; Förstner & Wittmann, 1981). PAHs are distributed in the environment in response to atmospheric transportation, wet and dry deposition, and surface-to-air exchange processes (Zhang et al., 2016).

PAHs are adsorbed on particles and end in the food chain due to their lipophilic and persistent nature, thereby causing carcinogenic, mutagenic, and teratogenic problems. Based on environment's authorities e.g. European Environment Agency (EEA) and the United States Environmental Protection Agency (US EPA) regulations, PAHs are listed as compounds that require elimination. Furthermore, based on the results of different researches on chronic impacts of PAHs, these compounds are categorized as an important part of endocrine disrupting compounds (EDCs) (Bergman et al., 2012; Wee and Aris, 2017; Yin et al., 2017; Zhang et al., 2016). Over the last few decades, the levels of PAHs have increased dramatically in the aquatic segments of ecosystem (Fechner, 2015; Forsgren, 2015; Shanker et al., 2017). Various methodologies have been developed for disposal of PAHs pollution in the atmosphere, soil, and sediment compartments. However, removal of the trace levels of PAHs from effluents have gained considerable attention in recent years regarding the fact that the effluent quality is a determinant factor in protecting aquatic life (Beach et al., 2010; National Academy of Sciences, 1993; Tjeerdema,

2012; Tornero and Hanke, 2016). Advanced oxidation processes (AOPs), which generate highly reactive hydroxyl radicals (e.g. ozonation, hydrogen peroxide applying, UV irradiation, and photocatalytic techniques) have been tested on pilot scale for the decomposition of various organic micropollutants in effluents (Pal et al., 2010).

In natural waters, degradation of PAHs partly happens owing to presence of oxidants (e.g. singlet oxygen, hydrogen peroxide, and hydroxyl radicals) and solar irradiation. Oxygenated PAHs are more reactive than their corresponding PAHs, so as a solution, applying AOPs as a post-treatment method for wastewaters ideally yield CO₂, H₂O, and inorganic compounds as final products (Daniela M. Pampanin, 2013; Kochany and Maguire, 1994; Ross and Crosby, 1985; Yan et al., 2004). In the case of catalytic processes for abatement of micropollutants in real matrices, various kinds of catalysts such as TiO₂, ZnO, Fe₂O₃, SnO₂, and CeO₂ have been employed in different studies (Oturán and Aaron, 2014). Due to exceptional stability under various conditions, the effective band gap energy (~3.2 eV), and relatively low price, TiO₂ has been widely investigated (Bagheri et al., 2017). In the present study, photocatalyst assisted tests were conducted on TiO₂ coated Pilkington Activ™ self-cleaning glass to eliminate the release of free nano-TiO₂ to the intended environment as secondary pollution after treatment (Battin et al., 2009; Deng et al., 2017; Mueller and Nowack, 2008; Stogiannidis and Laane, 2015; Wang et al., 2016). Photosensitized degradation by both visible and invisible light has been used for removing organic chemicals; in particular, increased efficiency of light-assisted degradation process has been proved via semiconducting of photocatalysis (Chatterjee and Mahata, 2002). In the present study, the photolytic degradation of naturally dissolved compounds of 16 EPA-Listed PAHs was compared in aqueous medium, under simulated natural sunlight by Xenon lamp irradiation and short-wavelength ultraviolet (UV-C100-280 nm) irradiation. Hydrogen peroxide was applied for generation of hydroxyl radical (OH•) to assist photolysis as a safe method for organic micropollutants removal from treated wastewater (Tiedeken et al., 2017). For all tests, the quantitative molecular structure of the remaining and degradation efficiency for target compounds were studied. The generated intermediates were also investigated. According to our knowledge, previous studies have not examined the mixture of 16 EPA-Listed PAHs and were focused on the degradation yields of more water soluble PAHs without presence of the other PAH congeners in the tests, whereas PAH concentrations in various environmental samples contains a mixture of lower molecular weight (LMW-PAHs) and high molecular weight (HMW-PAHs) even they are nonsoluble/semi-soluble in water, so the interaction between PAHs during AOP tests has remained ignored which is inevitable in real environment. The basic aim of this research is clarification of effective AOP methods which suits the requirements of green/sustainable water management.

MATERIAL AND METHODS

Preparation of aqueous PAHs solution

EPA 610 Polynuclear Aromatic Hydrocarbons Mixture analytical standard was obtained from Supelco (USA). The studied PAHs, along with their abbreviations, are listed in

Table 1. A total of 800 µL of the standard mixture was transferred to 2000 mL volumetric flasks containing approximately 300 mL deionized water. They were then marked by deionized water and shaken immediately to minimize glassware adsorption. The shaking continued up to complete disappearance of the droplets of the standard solution. The pH of the prepared solution was measured as 6.83 (concurrent temperature 25°C) by a WTW pH meter (model 3110, Germany). To achieve the most similar conditions to natural aqueous medium, surfactants were not applied to increase the solution of compounds. The solutions were stored under dark and cool conditions (4°C) until photodegradation processes. Stock solutions were prepared just before (30 minutes) experiments.

Photodegradation procedure

Characterization

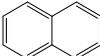
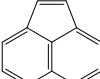
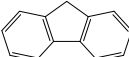
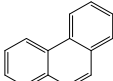
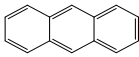
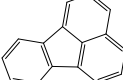
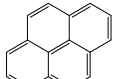
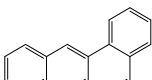
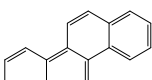
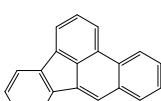
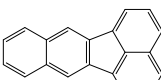
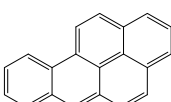
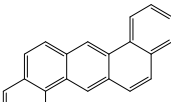
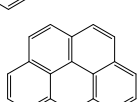
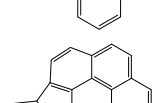
In order to determine the TiO₂ coated surface of the glass, size, and kind of particle which are key factors in photocatalyst efficiency (Gmurek et al., 2017), both surfaces of the Plinkton Active™ glass were characterized by Raman spectroscopy using (Renishaw InVia Raman spectroscopy RM1000, Gloucestershire, U.K.) as an accurate way for the analysis of surface morphology of thin TiO₂ films (Kurtoglu, Longenbach, and Gogotsi, 2011; Kurtoglu, Longenbach, Reddington, et al., 2011). The results of Raman spectra revealed clear characteristic peaks of anatase phase of TiO₂ nanocrystals (the Bands:144, 396, 514 and 636). The Raman spectra of glass surfaces are demonstrated in Figure 1a. X-ray diffraction patterns (XRD) were recorded by Bruker AXS model D8 advanced diffractometer (Cu Kα radiation (λ=1.54187 Å) at 40 kV and 35 mA with Bragg angle ranging from 3 to 70). Smoothed XRD image 2θ = 25.28° corresponding to the anatase phase TiO₂ is illustrated in Figure 1b. Regarding Scherrer equation and XRD results, the anatase phase of TiO₂ crystallite was determined too.

To clarify the roughness condition of the coated surface of Plinkton Active™ glass, the surface morphology of the glass was studied by atomic force microscopy (Flex AFM, Nanosurf, Switzerland). From the top-down view (TiO₂-coated surface of glass), the average TiO₂ nanoparticle diameter is about 90±30 nm (Figure 2.a). The hemispherical peaks are observable in the topographical view (Figure 2.b). From the sectional AFM view (Figure 2.d) the thickness of the TiO₂ layer on the glass is about 8±3 nm. The results indicate the appropriate roughness with a high surface area for the photocatalytically active surface of the glass. The top-down view (bare surface of glass) AFM images exhibit very smooth surface in comparison with the active surface (Figure 2.c).

The irradiation experiments used two UV-C TUV 15W lamps (model SLV/25, Phillips, Netherlands) and an Osram XBO R 300 WC Xe-arc lamp as a simulator of solar light. The radiation intensity of the UV lamp in the experimental setup was measured by UV radiometer (Cassy Lab Company, Germany).

After adjusting the distance of the active surface of glass and sources of irradiation, the light intensity was measured as 11.5 and 21.9 (W/m²) for UV-C and Xe tests, respectively.

Table 1. The physicochemical properties and abbreviations of studied PAHs

	PAH	Abbreviation	Structure	MW ^a (g.mol ⁻¹)	RN ^b	S ^c (mg.L ⁻¹)
1	Naphthalene	Nap		128	2	32
2	Acenaphthylene	Acy		152	3	3.9
3	Acenaphthene	Ace		152	3	3.9
4	Fluorene	Flu		166	3	1.9
5	Phenanthrene	Phe		178	3	1.1
6	Anthracene	Ant		178	3	0.05
7	Fluoranthene	Fln		202	4	0.26
8	Pyrene	Pyr		202	4	0.13
9	Benzo[a]anthracene	BaA		228	4	0.009–0.014
10	Chrysene	Cry		228	4	0.002
11	Benzo[b]fluoranthene	B[b]F		252	5	0.0014
12	Benzo[k]fluoranthene	B[k]F		252	5	0.0007–0.008
13	Benzo[a]pyrene	B[a]P		252	5	0.003
14	Dibenzo[a,h]anthracene	DBA		278	5	0.0005
15	Benzo[g,h,i]perylene	B[g,h,i]P		276	6	0.00026
16	Indeno[1,2,3-c,d]pyrene	Ind		276	6	0.00019

^a Molecular Weight, ^b Ring Number, ^c aqueous solubility (25 °C)

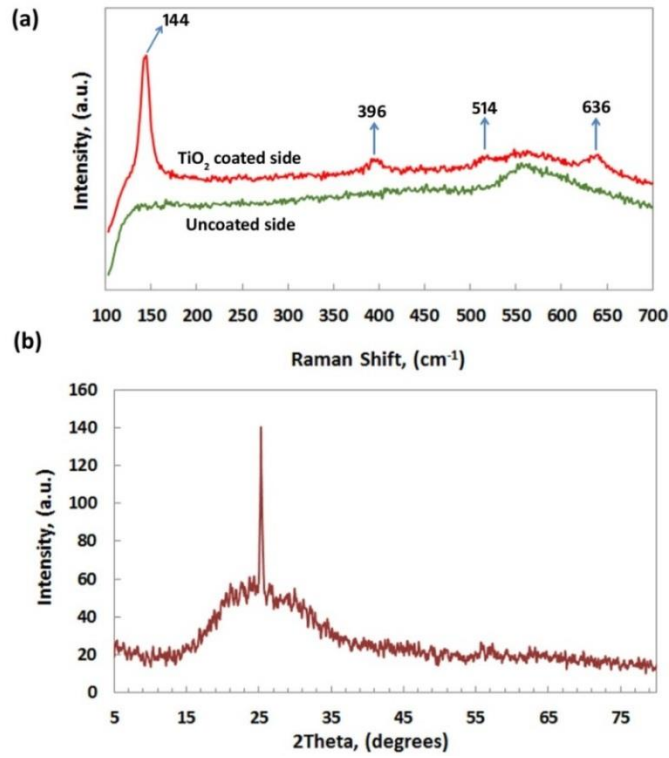


Figure 1. Raman spectra of glass surfaces (a) and XRD pattern of TiO₂ coated surface (b)

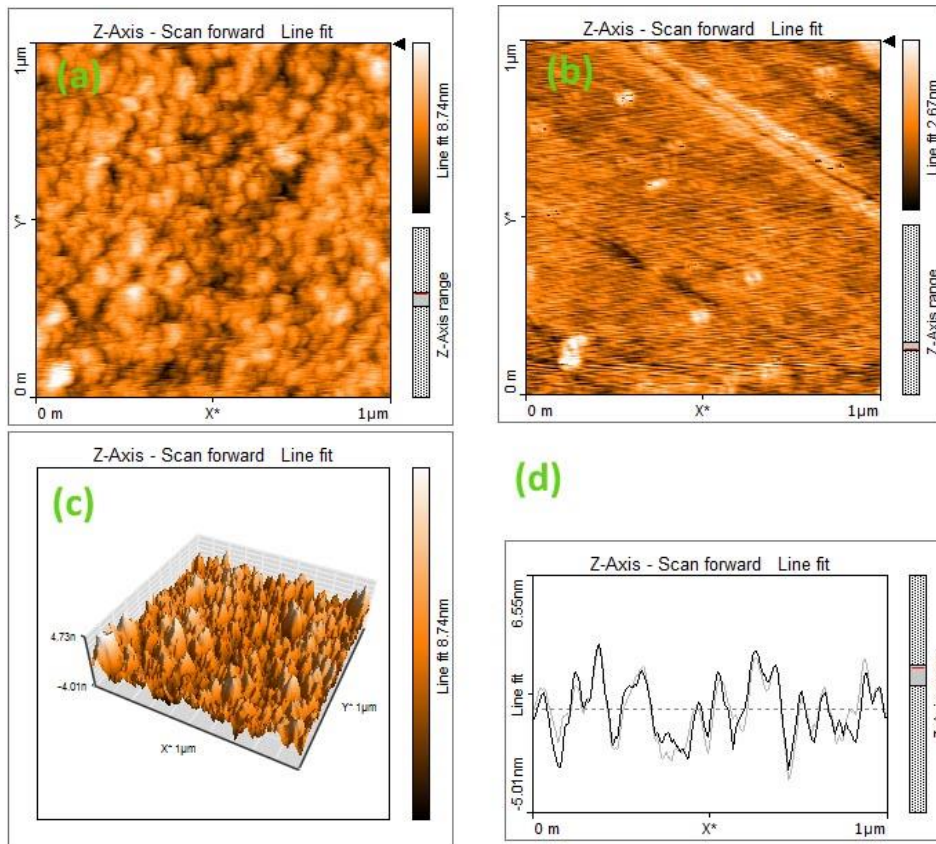


Figure 2. AFM images of Pilkington Activ™ glass in (a, b) a top-down view, (c) a topographical view, (d) sectional view for active and bar surfaces, respectively

Photodegradation procedure

Aqueous PAHs solution was poured into the Borosilicate 3.3 glass crystallization dishes (280 mL, Ø 95 mm) purchased from ISOLAB GmbH (Germany). Concerning UV-C/TiO₂ and Xe/TiO₂ tests, the round cut TiO₂ coated glass (Ø 75 mm) was placed in the crystallization dishes with nickel-chrome stands in direction of the irradiation sources. The active surface of the glass faced the lamps and aqueous PAHs solution was filled such that it rose about 1 cm from the active level of glass. Magnetic mini-stirrers model Topolino from IKA (Germany) and 6x25 mm PTFE magnetic stirring bars from LP ITALIANA S.p.A. (Italy) were used for agitating the solutions. To determine the concentration of H₂O₂ solution, titration with a 1 M solution of potassium permanganate (KMnO₄) was performed where the concentration was estimated at 31.19%. For UV-C/H₂O₂ and Xe/H₂O₂ tests, H₂O₂ concentration increased to 10 ppm by adding 2.2 µL H₂O₂ to 100 mL in the intended reaction vessels. Dark controls of the aqueous PAHs solution and H₂O₂-added solution were conducted to ensure that no loss of the PAHs occurred via reactions other than photolysis (i.e. hydrolysis, evaporation, and adsorption to the walls of the reaction vessel). Also, control adsorption experiments were performed for TiO₂-assisted tests.

The sampling was performed at times of 1, 2, 5 and 12 minutes after starting the irradiation across all tests. 15 mL of treated samples were taken by colorless polypropylene disposable pipet tips from BRAND™ (Germany) and stored in glass- screw cap conical centrifuge tubes with Rubber lined caps as a method of preventing evaporation from the samples; The tubes were washed carefully by GC-grade acetone and dried in 200°C for 30 min to eliminate any possible contaminations. Also, filled tubes covered with aluminium foil to prevent any light damage until extraction step. The reactor temperature was adjusted at 25°C for all tests. With regards to UV-C, UV-C/TiO₂, and UV-C/H₂O₂ tests, for each sampling, the electric source of the reactor was switched off to eliminate any possible exposure to UV-C irradiation. Also, considering volatility and high toxicity of the researched PAH compounds and an extraction solvent, wearing a NIOSH/MESA approved toxic gas respirator was necessary (USEPA, 2007).

Dispersive liquid-liquid microextraction (DLLME) procedure

Residual PAHs after the degradation process was determined gas chromatographically. For this purpose, an effective sample preparation was required. So, a dispersive liquid-liquid microextraction method as previously reported by Assadi *et al.* (Rezaee *et al.*, 2006) was employed with slight modifications. A 10.00 mL aqueous sample was placed in a 15 mL glass conical centrifuge tube. The mixture of 1.00 mL

of acetone (as disperser solvent) and 20.00 µL tetrachloroethylene (C₂Cl₄) (as extraction solvent) was injected into the sample. After formation of a stable cloudy solution, the mixture was centrifuged for 2 min at 6000 rpm. The dispersed solvent droplets were sedimented in the conical bottom of centrifuge tube. The 2.00 µL of sedimented phase was separated manually using a fixed needle syringe for Agilent Instruments (Thermo Scientific™) and stored in 100µL Insert silanized glass inserts/polymer spring/conical precision point interior placed in amber vials with cap PTFE/Silicone septa for GC and then samples transferred immediately to analyzed by GC/MS.

Chromatographic analyzes

The efficiency of the investigated method in the degradation of target compounds and identification of intermediate products during the degradation process were examined using gas chromatographic-mass spectrometric analysis. For this purpose, An Agilent 7890A GC coupled with 5975C MS (with EI source, Quadrupole mass analyzer, and triple axis detector) (USA) was utilized. Separation of PAHs and intermediate compounds was performed on Agilent HP-5MS capillary column (30 m × 0.25 mm ID, 1 µm film thickness) (USA) according to the following temperature programming:

The initial column temperature was set at 100 °C and held for 2 min then rose to 310 °C at 15 °C min⁻¹ and held for 25 min. Injection port, ionization source, and quadrupole mass analyzer temperatures were set at 280, 230 and 150 °C, respectively.

Quality assurance and quality control

The limits of detection (LODs) and limits of quantification (LOQs) are both important parameters as figures of merit in an analytical method which in chromatographic methods of analysis were calculated as 3×S/N and 10×S/N, respectively for each analyte (Table 2). The low LOD (7-10 ngL⁻¹) and LOQ (23-35 ngL⁻¹) values show high performance of the preferred analytical method in trace PAHs analysis. Also, linear dynamic range for each analyte was obtained by plotting calibration curve (analyte concentrations vs. corresponding peak areas) which started from concentrations near to LOQ and continues until 5% deviation from linearity. Good linearity ($r^2=0.9994-0.9999$) and wide linear dynamic range are advantages of the method. In order to evaluate the method precision, relative recoveries were calculated using added-found method via $R = \left(\frac{C_F}{C_A}\right) \times 100$, where CF and CA were the found concentration and added concentration of the analytes (EPA 610 Polynuclear Aromatic Hydrocarbons Mixture analytical standard), respectively. Results in Table 2, indicate that the results precision is acceptable.

Table 2. Figures of merit of DLLME-GC/MS method for PAHs analysis.

Compound	r^2	LOD (ngL ⁻¹)	LOQ (ngL ⁻¹)	LDR ^a (µgL ⁻¹)	Mean recovery(%)±SD ^b
Nap	0.9998	10	35	0.02-200	85.0±4.25
Acy	0.9997	10	35	0.02-200	82.5±4.54
Ace	0.9999	7	23	0.02-200	86.2±5.17
Flu	0.9995	8	26.5	0.02-200	87.1±4.79
Fln	0.9998	10	35	0.02-200	85.6±5.13
Pyr	0.9994	10	35	0.02-200	84.3±4.36

^aLinear Dynamic Range, ^b Standard Deviation

PAHs quantitative molecular profile fate

To clarify the quantitative molecular fate of PAHs profile in treated aqueous solutions, degradation efficiency (DE) of each PAH compound was evaluated under for all treatments. To elucidate the influence of studied AOPs on PAHs remaining profile, the total percentage of PAH remaining (\sum_6 PAHs) for each individual treatment were measured and compared. Also, to illustrate the properties of processes in terms of PAH content characteristics, PAH remaining was categorized according to their ring sequences.

Results and discussion

Dark control of the H₂O₂-added PAHs solution revealed negligible degradation values as 0.79, 1.00, 1.30 and 2.79% over the sampling time stages.

UV-C irradiated treatments

Degradation diagrams related to UV-C irradiated treatments are represented in [Figure 3](#).

Nap degradation pattern through UV-C treatment was recorded as 53.85, 54.88, 77.39, and 92.42% at 1, 2, 5, and 12 minutes after starting the treatment respectively. This pattern was recorded as 26.70, 4.72, 2.48 and 34.37% for UV-C/TiO₂ and 10.56, 27.91, 67.95, and 100.00% for UV-C/H₂O₂ treatment. In general, these results suggest high performance of UV-C and UV-C/H₂O₂ treatments in degradation of Nap. This compound has extensive applications and high solubility so presents predominantly in precipitations, effluents, and runoffs (see [Table 1](#)) ([Mastral and Callén, 2000](#); *Naphthalene in Moth Balls and Toilet Deodorant Cakes - Fact sheets*, n.d.; [Ravindra et al., 2008](#)). Based on this information, the researched AOPs seem more considerable for the degradation of Nap ([Mondal et al., 2014](#)).

The results of degradation pattern for Acy under UV-C treatment were 24.76, 12.97, 37.84, and 72.03% at 1, 2, 5 and 12 minutes after starting the treatment respectively. The degradation pattern of the abovementioned sampling times for UV-C/TiO₂ treatment was obtained as 29.20, -4.39, -10.50, and 24.40%. Also, 10.56, 27.91, 67.95, and 100.00% were identified for UV-C/H₂O₂. In general, high performance of UV-C/H₂O₂ in degradation of Acy was observed.

The degradation pattern of Ace was recorded as 29.04, 24.69, 53.89, and 81.40% for UV-C treatment; 32.63, 6.81, 0.73, and 26.40 for UV-C/TiO₂ treatment as well as 6.20, 69.70, 19.68, and 100.00% for UV-C/H₂O₂ treatment. The

results show high performance of UV-C/H₂O₂ in degradation of Ace.

Flu was degraded with 56.80, 59.29, 69.69, and 82.97% under UV-C treatment; 27.51, -12.63, -21.35 and 31.72% for UV-C/TiO₂ treatment and -2.23, 71.73, 25.06, and 100.00% for UV-C/H₂O₂ treatment. In general, high performance of UV-C/H₂O₂ treatment in degradation of Flu was evidenced.

The degradation pattern of Fln was recorded as: 100.00, -9.62, 100.00, and 100.00% under UV-C treatment, where 26.69, 22.95, 7.81, and 22.29% for UV-C/TiO₂ treatment and -2.18, 71.73, 25.07, and 100.00% through UV-C/H₂O₂ treatment were obtained. All these generally suggest the high performance of UV-C and UV-C/H₂O₂ treatments in degradation of Fln.

The results of degradation pattern of Pyr were identified as 39.84, 100.00, 100.00, and 53.66% under UV-C treatment; 100.00, 100.00, -25.89, and 12.85% for UV-C/TiO₂ treatment; and -2.18, 71.71, 25.08 and 100.00% for UV-C/H₂O₂ treatment. This group of results generally reveals high performance of UV-C/H₂O₂ treatment in degradation of Pyr.

Some minor exceptions (increases < -2% under UV-C/H₂O₂ treatments) are explainable by the low electrochemical oxidation potential of individual compounds Flu and Fln as 1.62 V and 1.83 V respectively ([Gurunathan et al., 1999](#)) in comparison with H₂O₂ oxidation potential of 2.8 V. Hence, H₂O₂ initially acts as an electron scavenger ([Viswanathan et al., 2015](#); "Water Treatability Database / Ultraviolet Irradiation + Hydrogen Peroxide," n.d.) up to production of OH• causing diminished DE over initial times of treatments (before 5 min).

In the [Figure 3.b](#) we are witness of increased peak of target compounds between sampling times of 1 min and 2 min in UV-C/TiO₂ test and then decrease the DE peaks in following sampling times, could be explained by catalytic cracking of PAHs via HMW-PAHs to LMW-PAHs during the process ([Pujro et al., 2015](#)) HMW-PAHs include compounds with five and six fused aromatic rings which are strongly carcinogenic and mutagenic. Further, due to the number of benzene rings and unsaturation degree they become increasingly stable and nonbiodegradable ([Stogiannidis and Laane, 2015](#)). HMW-PAHs are introduced into aquatic environments both directly (via dry deposition of aerosol-bound PAHs) ([González-Gaya et al., 2016](#)) and indirectly (through road and storm-water runoff) ([U.S. Environmental Protection Agency, 2007](#)). Accordingly, cracking the HMW-PAHs to lighter PAHs deserves attention.

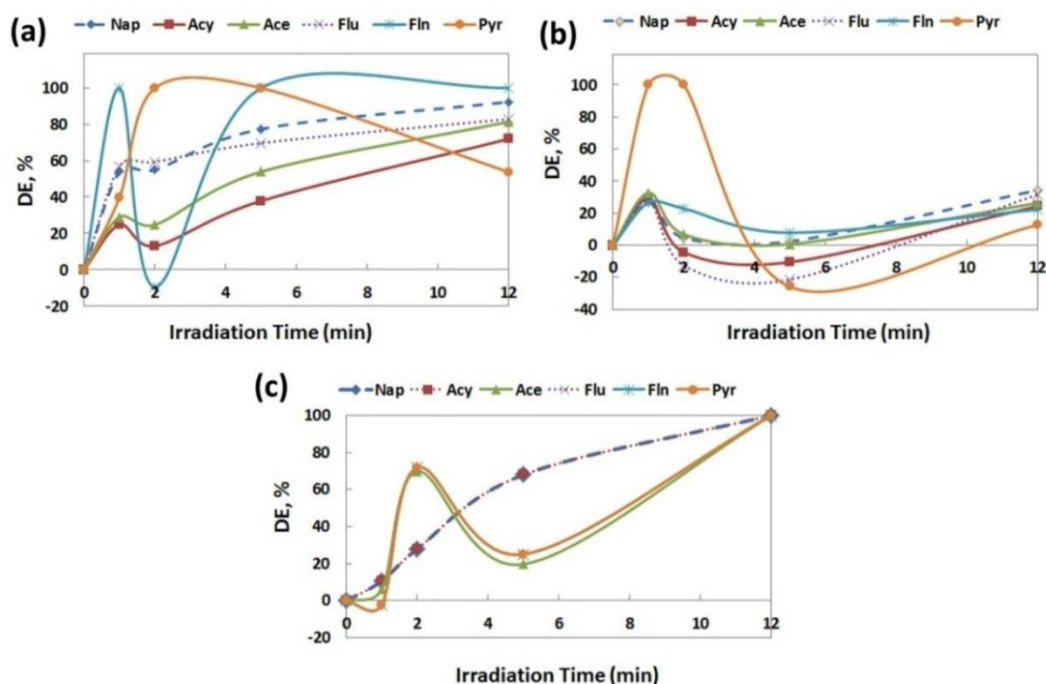


Figure 3. Degradation diagrams associated with UV-C irradiated treatments; UV-C treatment (a), UV-C/TiO₂ treatment (b), UV-C/H₂O₂ treatment (c)

Simulated solar treatments

Degradation diagrams related to Xe irradiated treatments are depicted in Figure 4.

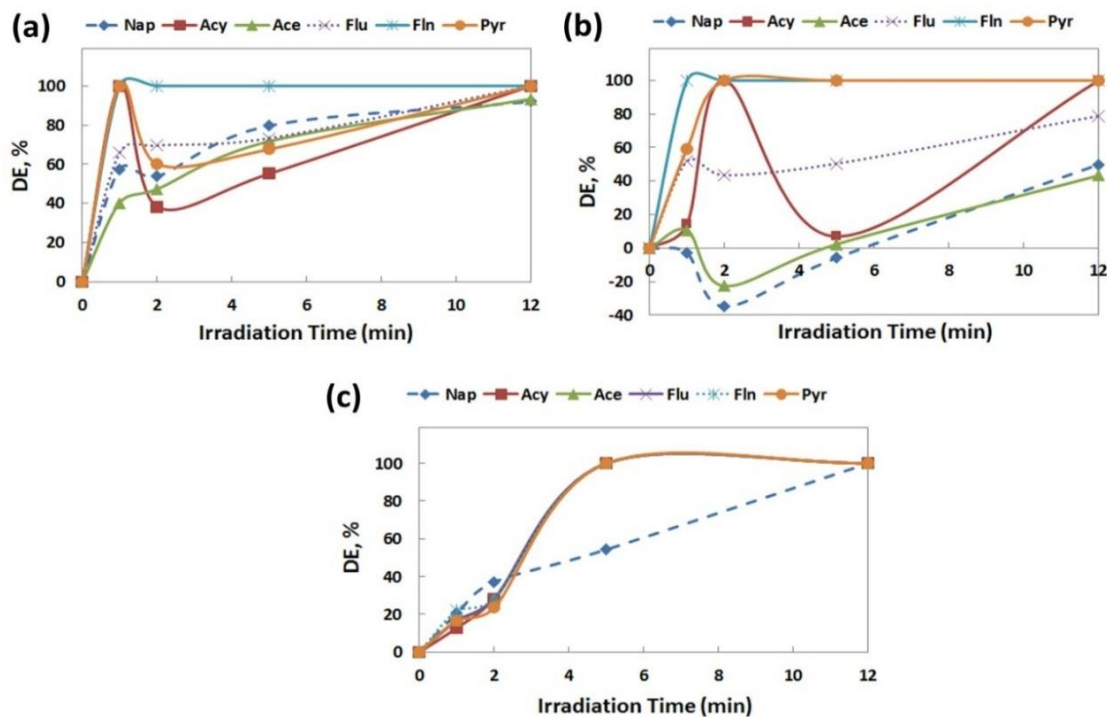


Figure 4. Degradation diagrams associated with the simulated solar irradiated treatments; Xe treatment (a), Xe/TiO₂ treatment (b), Xe/H₂O₂ treatment (c)

Nap degradation pattern was obtained as 57.55, 53.86, 79.71, and 92.08% by Xe irradiation treatment, where -3.08, -34.88, -5.83 and 49.92% for Xe/TiO₂ test as well as 20.48, 37.21, 54.36, and 100.00% for Xe/H₂O₂ treatment were achieved. The results suggest the high performance of Xe and Xe/H₂O₂ treatments in degradation of Nap. Observation of the increased peak of Nap at primary sampling times (1 and 2 min) of the Xe/TiO₂ treatment and stay undegraded (just 40% degraded) up to end of treatment (Figure 4.b) could be explained as catalytic cracking of PAHs by high molecular weight (HMW-PAHs) to lower molecular weight (LMW-PAHs) PAHs during the process (Pujro et al., 2015).

The results of degradation pattern for Acy were determined as 100.00, 38.48, 55.24, 100.00% for Xe irradiation treatment, where 14.34, 100.00, 6.94, and 100.00% for Xe/TiO₂ and 12.87, 28.34, 100.00, and 100.00% for Xe/H₂O₂ treatment were obtained. According to the results, high performance of UV-C/H₂O₂, Xe, and Xe /H₂O₂ treatments was evidenced in degradation of Acy. The Acy decreased 6.94% at min 5 subsequently 100% after min 2 under Xe/TiO₂ treatment, it could be explainable as catalytic cracking of PAHs by high molecular weight (HMW-PAHs) to lower molecular weight (LMW-PAHs) PAHs during the process too (Pujro et al., 2015).

Degradation pattern of Ace recorded as: 40.37, 47.39, 71.75 and 93.36 degradation percentages for Xe irradiation treatment; 10.63, -22.64, 2.35 and 43.32 percentages for Xe/TiO₂ treatment and 16.73, 28.21, 100.00 and 100.00 percentages were obtained for Xe/H₂O₂ at 1, 2, 5 and 12 minutes after starting the treatment. Regarding this group of

results, Xe and Xe/H₂O₂ treatments were revealed high performance to degradation of Ace.

The degradation pattern of Flu was recorded as: 65.87, 69.59, 73.31, and 100.00% through Xe irradiation treatment, where 51.78, 43.50, 50.47, and 78.83% for Xe/TiO₂ treatment and 16.74, 28.29, 100.00, and 100.00% for Xe/H₂O₂ were obtained at 1, 2, 5 and 12 minutes after starting the treatment. In general, Xe and Xe/H₂O₂ treatments exhibited high performance in the case of Flu degradation.

The results of degradation pattern for Fln revealed 100.00% at all sampling steps under Xe irradiation and Xe/TiO₂-assisted treatments. Also, 21.97, 28.32, 100.00, and 100.00% for Xe/H₂O₂ were determined at 1, 2, 5, and 12 minutes after starting the treatment. This group of results generally indicates the high performance of Xe, Xe/H₂O₂, and Xe/TiO₂ treatments in degradation of Fln.

The results of degradation pattern of Pyr were identified as 100.00, 60.19, 67.70 and 100.00% for Xe through treatment at 1, 2, 5 and 12 minutes after starting the treatment. Also, 59.26% of the first sampling stage and 100.00% of the next sampling time stages were obtained under solar-TiO₂ assisted treatment, while 16.79, 23.57, 100.00, and 100.00% were achieved for Xe/H₂O₂ at sampling time steps. These results generally suggest the high performance of Xe, Xe/H₂O₂, and Xe/TiO₂ treatments in degradation of Pyr.

Total PAH remaining pattern

The survey of total mass remains of PAH for each individual treatment has been reported in Figure 5.

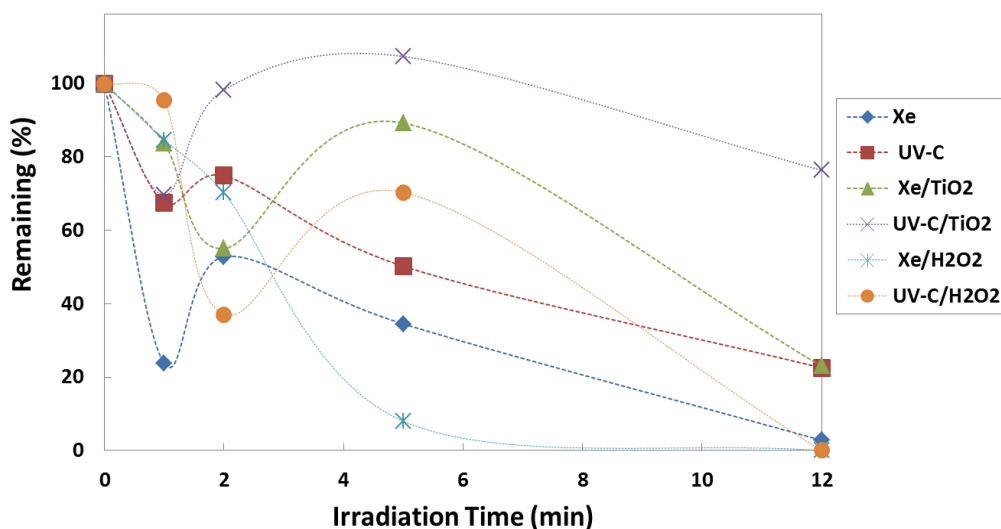


Figure 5. Σ 6 PAHs remaining diagram for investigated AOPs

As presented in the diagram, apparently DE in TiO₂-assisted treatments seems very weak (total remaining of 76.38% after 12-min treatment). This can be explained by lower energy band gap of PAHs with lower molecular weight (2-4 ringed PAHs) (Luo et al., 2015). Further, the limited amount of coated TiO₂ nanocrystals on the glass is another possible reason for seemingly weaker performances in comparison with other treatment processes. With growth in the active surface of TiO₂ and/or increase the treatment duration, enhancement of degradation rate will be expectable (D. Dionysiou et al., 2016). Overall, the total six parent PAHs concentrations in the last sampling stage (12 min after

starting the treatment) can be ranked as follows: UV-C/TiO₂ > Xe/TiO₂ > UV-C > Xe > Xe/H₂O₂, and UV-C /H₂O₂ with estimated values of 76.38, 23.02, 22.55, 2.78, 0.00 and 0.00% of the concentration values at the beginning of the treatment, respectively.

Ring sequencing

The remaining PAHs were categorized according to their ring sequences, as two-ring group (including Nap), three-ring group (including Acy, Ace, and Flu) and four-ring group (including Flt and Pyr) (Figures 6 and 7).

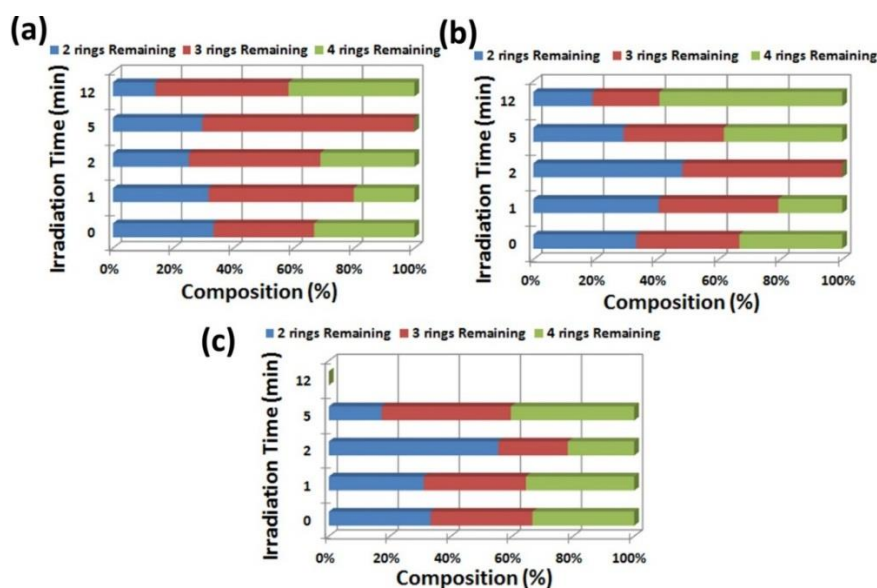


Figure 6. Remaining concentration composition of PAHs categorized according to their ring sequences for UV-C treatment (a), UV-C/TiO₂ treatment (b), and UV-C/H₂O₂ treatment (c)

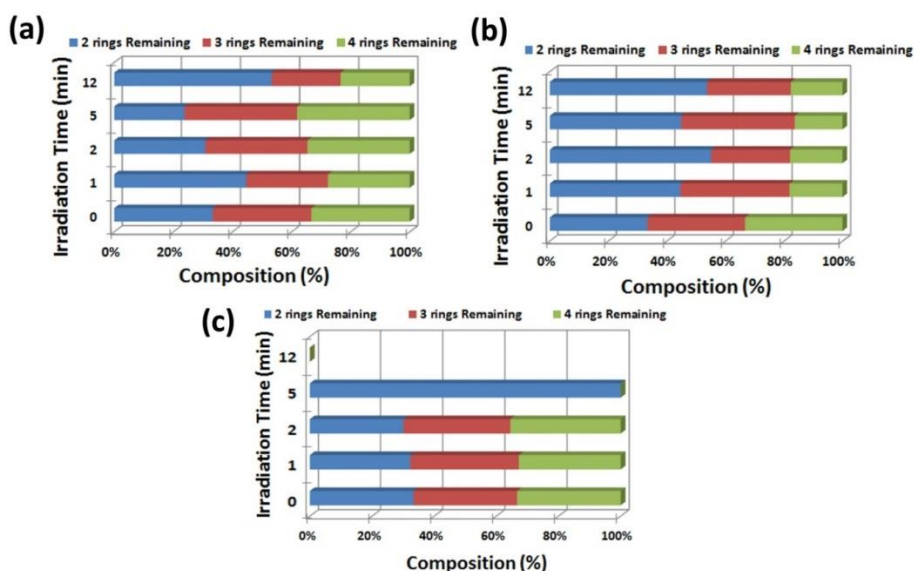


Figure 7. Remaining concentration composition of the PAHs categorized according to their ring sequences for Xe treatment (a), Xe/TiO₂ treatment (b), and Xe/H₂O₂ treatment (c)

Regarding the diagrams of remaining PAH patterns with reference to their ring sequences, we witnessed an ascending trend in 2 rings remaining in PAHs profiles belonging to solar irradiated treatments (Xe, Xe/H₂O₂, and Xe/ TiO₂) although the reverse was recorded for UV-C treated tests (UV-C, UV-C /H₂O₂, and UV-C / TiO₂). These results suggest the absolutely high performance of Xe/H₂O₂ (Figure 7.c) and UV-C/H₂O₂ (Figure 6.c) treatment for abatement of the parent target PAH compounds (100% at 12 min after starting the treatment) but from the view of the ring sequences of remaining concentration at 5th min of treatment in Xe/H₂O₂ and UV-C/H₂O₂ treatments, Xe/H₂O₂ profile is superior to UV-C/H₂O₂. Converting the profile of PAHs in aqueous mixture with both “petrogenic” and “pyrogenic” characteristics to lighter petrogenic characteristic is desirable in terms of environmental health globally (Ramesh et al., 2011). However, there is a need to extend ecotoxicological tests to achieve reliable information about the environmental applicability of the AOPs in real scale regarding the high possibility of generation of hydroxy-PAHs (OH-PAHs) in H₂O₂-assisted treatments due to a significant reduction factor of OH•. The polar functional groups enhance the hydrophilicity of OH-PAHs (Achten and Andersson, 2015). Also, some OH-PAHs have higher genotoxicity and higher half-live with more persistent, bioaccumulative and toxic properties (Motorykin et al., 2015).

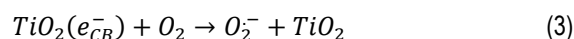
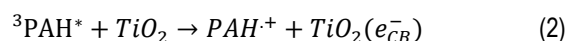
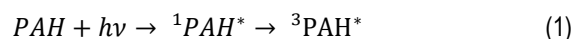
Formation of temporary products

For the investigated processes including UV, Xe, UV/TiO₂, Xe/TiO₂, UV/H₂O₂, and Xe/H₂O₂, the remaining temporary byproducts were determined after 12 min of each process. The experiments were repeated for three times with repetitious GC peaks analyzed. The identified byproducts are reported in Table 3. During PAHs photodegradation under UV and Xenon irradiations, sequencing destruction of PAHs leads to the formation of compounds 1 and 3. Other byproducts containing oxygenated functional groups can be produced by the general following pathways (Fasnacht and Blough, 2003):

The PAHs photodegradation can initiate by three proposed primary reactions. In the first pathway, the absorption of a photon by PAH molecule results in the generation of PAH cation-radical (PAH⁺) thereby releasing an electron reacting with dissolved oxygen molecule (Miller and Olejnik, 2001). The generated cation-radicals can produce very oxidative radical intermediates such as superoxide anion-radicals and aromatic hydrocarbon anion radicals from reacting with water molecules or hydroxide anions. The produced radicals can further react with PAHs to produce stable byproducts containing oxygenated functional groups listed in Table 3. The active oxidative radicals can be produced via other mechanisms. The second pathway involves development of excited triplet state of a PAH

molecule with O₂ in a ³PAH^{*}-³O₂ complex (Sigman et al., 1991). It has also been proposed that O₂ can be adsorbed by a PAH molecule to form a ground state PAH-O₂ complex. Under the photon irradiation, charge transfer complex will be formed (photoionization). PAH⁺ - O₂⁻ complex can produce superoxide anion-radicals (Sigman et al., 1998).

During advanced oxidation processes (i.e UV/TiO₂, Xe/TiO₂, UV/H₂O₂ processes), it is well known very oxidative and highly reactive hydroxyl radicals are generated (Amani-Ghadim and Dorraji, 2015) which can oxidize the organic pollutants unselectively. These relevant reactions at the photocatalyst surface cause the degradation of PAHs. In addition to the mentioned reactions, for producing hydroxyl radicals, the active radicals can be generated via photosensitization mechanism described in Eqs. (1-3) (Konstantinou and Albanis, 2004):



Due to the non-selective reaction feature of hydroxyl radicals, formation of various by-products is expectable. However, it is very difficult to determine the degradation pathway of each PAH and the parent PAH of each identified byproduct. With change the main GC peaks related to the PAHs, some new peaks related to temporary degradation byproducts were appeared.

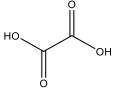
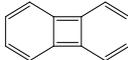
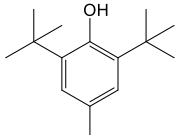
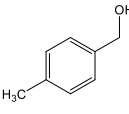
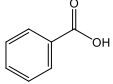
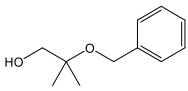
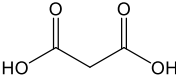
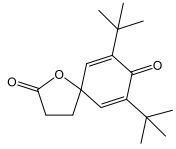
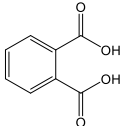
CONCLUSIONS

This study investigated the photochemical treatments based on simulated solar and UV-C radiation with TiO₂ and H₂O₂ for degradation of dissolved compounds of 16 EPA-Listed PAHs in aqueous medium. During simulated solar treatment processes, the structure of residual PAHs was changed and the ratio of lighter compounds (2,3-ringed PAHs) increased clearly before accomplishment of the removal process. The results have expanded the borders of understanding on the fate of PAHs and their by-products in aqueous medium through the investigated AOPs, which facilitated the prediction of PAH-related hazards in aqueous medium. Multistage treatment system approaches, end to bioremediation systems to decay trace, light and biodegradable remaining can be supposed to reinforce AOP water treatment systems to achieve high levels of environmental safety for effluents of the system. The results suggested the ability of solar irradiation to reduce PAH pollution in contaminated effluents and superiority of PAH-degrading of Xe/H₂O₂ and UV-C/H₂O₂ treatment for total

elimination of parent PAH contaminants in aqueous medium. Undoubtedly, performing future extended ecotoxicological

tests can expand the real scale tests to decrease the influence of PAHs on aquatic environments.

Table 3. Possible identified byproducts during photolytic degradation of naturally dissolved compounds of 16 EPA-Listed PAHs by UV, Xe, UV-TiO₂, Xe-TiO₂, UV/H₂O₂, and Xe/H₂O₂ processes

Compound	Retention time (min)	Main fragments	Product Structure	Product Name	Process
1	7.145	78, 77, 52, 51, 39		Benzene	Xenon, UV
2	7.848	46, 44, 29, 28, 18		Oxalic acid	Xenon, Xenon/TiO ₂ coated glass, Xenon/H ₂ O ₂
3	10.065	152, 126, 76, 63, 50		Biphenylene	Xenon, UV, Xenon/TiO ₂ coated glass
4	10.205	94, 66, 40, 39		Phenol	All investigated processes
5	10.307	220, 205, 189, 177, 161, 145, 57		Butylated hydroxytoluene	UV-TiO ₂ coated glass UV/H ₂ O ₂
6	11.021	122, 107, 91, 79, 65, 39		4-Methylbenzyl alcohol	UV
7	11.309	122, 105, 94, 77, 51, 39, 27		Benzoic acid	All investigated processes
8	11.537	107, 92, 91		2-(Benzyloxy)-2-methylpropan-1-ol	UV
9	12.597	87, 60, 45, 43, 42, 29		Malonic acid	All investigated processes
10	13.495	276, 261, 232, 217, 205, 189, 175, 161, 149, 135, 109, 91, 57		7,9-Di-tert-butyl-1-oxaspiro(4,5)deca-6,9-diene-2,8-dione	Xenon/TiO ₂ coated glass UV
11	17.286	148, 104, 76, 50, 38, 18		1,2-benzenedicarboxylic acid	All investigated processes

ACKNOWLEDGMENTS

This study was partially funded by Ege University Scientific Research (BAP) (Project No.: 2017/SÜF/014). Authors acknowledge Dr. Ozan Ünsalan (Ege University, Department of Physics) for his help with the analysis of

Raman spectra. Navid Kargar and Golnar Matin thank Prof. Yury Gogotsi (A.J. Drexel Nanotechnology Institute, Drexel University) for his useful comments and suggestions on characterization of TiO₂ nanocrystals.

REFERENCES

- Achten, C. & Andersson, J.T. (2015). Overview of Polycyclic Aromatic Compounds (PAC). *Polycyclic Aromatic Compounds*, 35(2-4), 177-186. DOI: [10.1080/10406638.2014.994071](https://doi.org/10.1080/10406638.2014.994071)
- Amani-Ghadim, A.R. & Dorraji, M.S.S. (2015). Modeling of photocatalytic process on synthesized ZnO nanoparticles: Kinetic model development and artificial neural networks. *Applied Catalysis B: Environmental*, 163, 539-546. DOI: [10.1016/j.apcatb.2014.08.020](https://doi.org/10.1016/j.apcatb.2014.08.020)
- Bagheri, S., Termehyousefi, A. & Do, T.O. (2017). Photocatalytic pathway toward degradation of environmental pharmaceutical pollutants: Structure, kinetics and mechanism approach. *Catalysis Science and Technology*, 7(20), 4548-4569. DOI: [10.1039/c7cy00468k](https://doi.org/10.1039/c7cy00468k)
- Battin, T.J., Kammer, F. v.d., Weilharter, A., Ottofuelling, S. & Hofmann, T. (2009). Nanostructured TiO₂: Transport Behavior and Effects on Aquatic Microbial Communities under Environmental Conditions. *Environmental Science & Technology*, 43(21), 8098-8104. DOI: [10.1021/es9017046](https://doi.org/10.1021/es9017046)
- Beach, D. G., Quilliam, M. A., Rouleau, C., Croll, R.P. & Hellou, J. (2010). Bioaccumulation and biotransformation of pyrene and 1-hydroxypyrene by the marine whelk *Buccinum undatum*. *Environmental Toxicology and Chemistry*, 29(4), 779-788. DOI: [10.1002/etc.112](https://doi.org/10.1002/etc.112)
- Bergman, Å., Heindel, J., Jobling, S., Kidd, K. & Zoeller, R.T. (2012). *State of the science of endocrine disrupting chemicals, 2012*. *Toxicology Letters* (Vol. 211). UNEP/WHO. DOI: [10.1016/j.toxlet.2012.03.020](https://doi.org/10.1016/j.toxlet.2012.03.020)
- Chatterjee, D. & Mahata, A. (2002). Visible light induced photodegradation of organic pollutants on dye adsorbed TiO₂ surface. *Journal of Photochemistry and Photobiology A: Chemistry*, 153(1-3), 199-204. DOI: [10.1016/S1010-6030\(02\)00291-5](https://doi.org/10.1016/S1010-6030(02)00291-5)
- Daniela, M. Pampanin, M.O.S. (2013). Polycyclic Aromatic Hydrocarbons a Constituent of Petroleum: Presence and Influence in the Aquatic Environment. In *Hydrocarbon*. InTech. DOI: [10.5772/48176](https://doi.org/10.5772/48176)
- Deng, X.-Y., Cheng, J., Hu, X.-L., Wang, L., Li, D. & Gao, K. (2017). Biological effects of TiO₂ and CeO₂ nanoparticles on the growth, photosynthetic activity, and cellular components of a marine diatom *Phaeodactylum tricornutum*. *Science of The Total Environment*, 575, 87-96. DOI: [10.1016/j.scitotenv.2016.10.003](https://doi.org/10.1016/j.scitotenv.2016.10.003)
- Dionysiou, D., Puma, G.L., Ye, J., Schneider, J. & Bahnemann, D. (2016). *Photocatalysis Applications*. (D. D. Dionysiou, G. Li Puma, J. Ye, J. Schneider, & D. Bahnemann, Eds.). Cambridge: Royal Society of Chemistry. DOI: [10.1039/9781782627104](https://doi.org/10.1039/9781782627104)
- Fasnacht, M.P. & Blough, N.V. (2003). Mechanisms of the Aqueous Photodegradation of Polycyclic Aromatic Hydrocarbons. *Environmental Science & Technology*, 37(24), 5767-5772. DOI: [10.1021/es034389c](https://doi.org/10.1021/es034389c)
- Fechner, H.F.H. & E.J. (2015). *Chemical Fate and Transport in the Environment*. Elsevier. DOI: [10.1016/C2011-0-09677-1](https://doi.org/10.1016/C2011-0-09677-1)
- Forsgren, A.J. (2015). *Wastewater Treatment: Occurrence and Fate of Polycyclic Aromatic Hydrocarbons (PAHs)*. CRC Press. Retrieved from [https://books.google.com.tr/books?id=D3V3CAAAQBAJ&dq=Wastewater+Treatment+Occurrence+and+Fate+of+Polycyclic+Aromatic+Hydrocarbons+\(PAHs\)+DIO&lr=&source=gbs_navlinks_s&hl=en](https://books.google.com.tr/books?id=D3V3CAAAQBAJ&dq=Wastewater+Treatment+Occurrence+and+Fate+of+Polycyclic+Aromatic+Hydrocarbons+(PAHs)+DIO&lr=&source=gbs_navlinks_s&hl=en)
- Förstner, U. & Wittmann, G.T.W. (1981). *Metal Pollution in the Aquatic Environment*. Springer-Verlag. DOI: [10.1007/978-3-642-69385-4](https://doi.org/10.1007/978-3-642-69385-4)
- Gmurek, M., Olak-Kucharczyk, M. & Ledakowicz, S. (2017). Photochemical decomposition of endocrine disrupting compounds – A review. *Chemical Engineering Journal*, 310, 437-456. DOI: [10.1016/j.cej.2016.05.014](https://doi.org/10.1016/j.cej.2016.05.014)
- González-Gaya, B., Fernández-Pinos, M.-C., Morales, L., Méjanelle, L., Abad, E., Piña, B., ... Dachs, J. (2016). High atmosphere-ocean exchange of semivolatile aromatic hydrocarbons. *Nature Geoscience*, 9(6), 438-442. DOI: [10.1038/ngeo2714](https://doi.org/10.1038/ngeo2714)
- Gurunathan, K., Murugan, A.V., Marimuthu, R., Mulik, U. & Amalnerkar, D. (1999). Electrochemically synthesised conducting polymeric materials for applications towards technology in electronics, optoelectronics and energy storage devices. *Materials Chemistry and Physics*, 61(3), 173-191. DOI: [10.1016/S0254-0584\(99\)00081-4](https://doi.org/10.1016/S0254-0584(99)00081-4)
- Kochany, J. & Maguire, R.J. (1994). Abiotic transformations of polynuclear aromatic hydrocarbons and polynuclear aromatic nitrogen heterocycles in aquatic environments. *Science of The Total Environment*, 144(1-3), 17-31. DOI: [10.1016/0048-9697\(94\)90424-3](https://doi.org/10.1016/0048-9697(94)90424-3)
- Konstantinou, I.K. & Albanis, T.A. (2004). TiO₂-assisted photocatalytic degradation of azo dyes in aqueous solution: kinetic and mechanistic investigations. *Applied Catalysis B: Environmental*, 49(1), 1-14. DOI: [10.1016/j.apcatb.2003.11.010](https://doi.org/10.1016/j.apcatb.2003.11.010)
- Kurtoglu, M. E., Longenbach, T. & Gogotsi, Y. (2011). Preventing Sodium Poisoning of Photocatalytic TiO₂ Films on Glass by Metal Doping. *International Journal of Applied Glass Science*, 2(2), 108-116. DOI: [10.1111/j.2041-1294.2011.00040.x](https://doi.org/10.1111/j.2041-1294.2011.00040.x)
- Kurtoglu, M. E., Longenbach, T., Reddington, P. & Gogotsi, Y. (2011). Effect of Calcination Temperature and Environment on Photocatalytic and Mechanical Properties of Ultrathin Sol-Gel Titanium Dioxide Films. *Journal of the American Ceramic Society*, 94(4), 1101-1108. DOI: [10.1111/j.1551-2916.2010.04218.x](https://doi.org/10.1111/j.1551-2916.2010.04218.x)
- Luo, Z., Wei, C., He, N., Sun, Z., Li, H. & Chen, D. (2015). Correlation between the Photocatalytic Degradability of PAHs over Pt/TiO₂-SiO₂ in Water and Their Quantitative Molecular Structure. *Journal of Nanomaterials*, 2015, 1-11. DOI: [10.1155/2015/284834](https://doi.org/10.1155/2015/284834)
- Mastral, A.M. & Callén, M.S. (2000). A Review on Polycyclic Aromatic Hydrocarbon (PAH) Emissions from Energy Generation. *Environmental Science & Technology*, 34(15), 3051-3057. DOI: [10.1021/es001028d](https://doi.org/10.1021/es001028d)
- Miller, J.S., & Olejnik, D. (2001). Photolysis of polycyclic aromatic hydrocarbons in water. *Water Research*, 35(1), 233-243. DOI: [10.1016/S0043-1354\(00\)00230-X](https://doi.org/10.1016/S0043-1354(00)00230-X)
- Mondal, K., Bhattacharyya, S. & Sharma, A. (2014). Photocatalytic Degradation of Naphthalene by Electrospun Mesoporous Carbon-Doped Anatase TiO₂ Nanofiber Mats. *Industrial & Engineering Chemistry Research*, 53(49), 18900-18909. DOI: [10.1021/ie5025744](https://doi.org/10.1021/ie5025744)
- Motorykin, O., Santiago-Delgado, L., Rohlman, D., Schrlau, J. E., Harper, B., Harris, S., ... Massey Simonich, S. L. (2015). Metabolism and excretion rates of parent and hydroxy-PAHs in urine collected after consumption of traditionally smoked salmon for Native American volunteers. *Science of The Total Environment*, 514, 170-177. DOI: [10.1016/j.scitotenv.2015.01.083](https://doi.org/10.1016/j.scitotenv.2015.01.083)
- Mueller, N.C. & Nowack, B. (2008). Exposure Modeling of Engineered Nanoparticles in the Environment. *Environmental Science & Technology*, 42(12), 4447-4453. DOI: [10.1021/es7029637](https://doi.org/10.1021/es7029637)
- Naphthalene in Moth Balls and Toilet Deodorant Cakes - Fact sheets*. (n.d.). Retrieved from www.health.nsw.gov.au/publichealth/infectious/plus.asp
- National Academy of Sciences. (1993). *Managing Wastewater in Coastal Urban Areas*. Washington, D.C.: National Academies Press. DOI: [10.17226/2049](https://doi.org/10.17226/2049)
- Oturan, M.A. & Aaron, J.-J. (2014). Advanced Oxidation Processes in Water/Wastewater Treatment: Principles and Applications. A Review. *Critical Reviews in Environmental Science and Technology*, 44(23), 2577-2641. DOI: [10.1080/10643389.2013.829765](https://doi.org/10.1080/10643389.2013.829765)
- Pal, A., Gin, K.Y.H., Lin, A.Y.C. & Reinhard, M. (2010). Impacts of emerging organic contaminants on freshwater resources: Review of recent occurrences, sources, fate and effects. *Science of the Total Environment*, 408(24), 6062-6069. DOI: [10.1016/j.scitotenv.2010.09.026](https://doi.org/10.1016/j.scitotenv.2010.09.026)
- Pujro, R., Falco, M. & Sedran, U. (2015). Catalytic Cracking of Heavy Aromatics and Polycyclic Aromatic Hydrocarbons over Fluidized Catalytic Cracking Catalysts. *Energy & Fuels*, 29(3), 1543-1549. DOI: [10.1021/ef502707w](https://doi.org/10.1021/ef502707w)
- Ramesh, A., Archibong, A., Hood, D., Guo, Z. & Loganathan, B. (2011). Global Environmental Distribution and Human Health Effects of Polycyclic Aromatic Hydrocarbons. In *Global Contamination Trends of Persistent Organic Chemicals* (pp. 97-126). CRC Press. DOI: [10.1201/b11098-7](https://doi.org/10.1201/b11098-7)
- Ravindra, K., Sokhi, R. & Van Grieken, R. (2008). Atmospheric polycyclic aromatic hydrocarbons: Source attribution, emission factors and regulation. *Atmospheric Environment*, 42(13), 2895-2921. DOI: [10.1016/j.atmosenv.2007.12.010](https://doi.org/10.1016/j.atmosenv.2007.12.010)
- Rezaee, M., Assadi, Y., Milani Hosseini, M.-R., Aghaee, E., Ahmadi, F. & Berijani, S. (2006). Determination of organic compounds in water using dispersive liquid-liquid microextraction. *Journal of Chromatography A*, 1116(1-2), 1-9. <http://doi.org/10.1016/j.chroma.2006.03.007>

- Ross, R.D. & Crosby, D.G. (1985). Photooxidant activity in natural waters. *Environmental Toxicology and Chemistry*, 4(6), 773–778. DOI: [10.1002/etc.5620040608](https://doi.org/10.1002/etc.5620040608)
- Shanker, U., Jassal, V. & Rani, M. (2017). Degradation of toxic PAHs in water and soil using potassium zinc hexacyanoferrate nanocubes. *Journal of Environmental Management*, 204, 337–348. DOI: [10.1016/j.jenvman.2017.09.015](https://doi.org/10.1016/j.jenvman.2017.09.015)
- Sigman, M.E., Schuler, P.F., Ghosh, M.M. & Dabestani, R.T. (1998). Mechanism of Pyrene Photochemical Oxidation in Aqueous and Surfactant Solutions. *Environmental Science & Technology*, 32(24), 3980–3985. DOI: [10.1021/es9804767](https://doi.org/10.1021/es9804767)
- Sigman, M.E., Zingg, S.P., Pagni, R.M. & Burns, J. H. (1991). Photochemistry of anthracene in water. *Tetrahedron Letters*, 32(41), 5737–5740. DOI: [10.1016/S0040-4039\(00\)93543-3](https://doi.org/10.1016/S0040-4039(00)93543-3)
- Stogiannidis, E. & Laane, R. (2015). Source Characterization of Polycyclic Aromatic Hydrocarbons by Using Their Molecular Indices: An Overview of Possibilities. In *Springer International Publishing* (Vol. 234, pp. 49–133). Springer International Publishing . DOI: [10.1007/978-3-319-10638-0_2](https://doi.org/10.1007/978-3-319-10638-0_2)
- Tiedeken, E.J., Tahar, A., McHugh, B. & Rowan, N.J. (2017). Monitoring, sources, receptors, and control measures for three European Union watch list substances of emerging concern in receiving waters – A 20 year systematic review. *Science of The Total Environment*, 574, 1140–1163. DOI: [10.1016/j.scitotenv.2016.09.084](https://doi.org/10.1016/j.scitotenv.2016.09.084)
- Tjeerdema, R.S. (2012). *Aquatic Life Water Quality Criteria for Selected Pesticides*. (R. S. Tjeerdema, Ed.) (Vol. 216). Boston, MA: Springer US. DOI: [10.1007/978-1-4614-2260-0](https://doi.org/10.1007/978-1-4614-2260-0)
- Tornero, V., & Hanke, G. (2016). Chemical contaminants entering the marine environment from sea-based sources: A review with a focus on European seas. *Marine Pollution Bulletin*, 112(1–2), 17–38. DOI: [10.1016/j.marpolbul.2016.06.091](https://doi.org/10.1016/j.marpolbul.2016.06.091)
- U.S. Environmental Protection Agency. (2007). *Ecological Soil Screening Levels for Polycyclic Aromatic Hydrocarbons (PAHs) Interim Final*. Washington, DC. Retrieved from https://www.epa.gov/sites/production/files/2015-09/documents/eco-ssl_pah.pdf
- USEPA. (2007). *Method 625 - Base/Neutrals and Acids. Methods for organic chemical analysis of municipal and industrial wastewater*.
- Viswanathan, V., Hansen, H.A., & Nørskov, J.K. (2015). Selective Electrochemical Generation of Hydrogen Peroxide from Water Oxidation. *The Journal of Physical Chemistry Letters*, 6(21), 4224–4228. DOI: [10.1021/acs.jpcllett.5b02178](https://doi.org/10.1021/acs.jpcllett.5b02178)
- Wang, Y., Zhu, X., Lao, Y., Lv, X., Tao, Y., Huang, B., ... Cai, Z. (2016). TiO₂ nanoparticles in the marine environment: Physical effects responsible for the toxicity on algae *Phaeodactylum tricornutum*. *Science of The Total Environment*, 565, 818–826. DOI: [10.1016/j.scitotenv.2016.03.164](https://doi.org/10.1016/j.scitotenv.2016.03.164)
- Water Treatability Database / Ultraviolet Irradiation + Hydrogen Peroxide. (n.d.). Retrieved December 26, 2018, from <https://iaspub.epa.gov/tdb/pages/treatment/treatmentOverview.do>
- Wee, S.Y. & Aris, A.Z. (2017). Endocrine disrupting compounds in drinking water supply system and human health risk implication. *Environment International*, 106(April), 207–233. DOI: [10.1016/j.envint.2017.05.004](https://doi.org/10.1016/j.envint.2017.05.004)
- Yan, J., Wang, L., Fu, P.P. & Yu, H. (2004). Photomutagenicity of 16 polycyclic aromatic hydrocarbons from the US EPA priority pollutant list. *Mutation Research/Genetic Toxicology and Environmental Mutagenesis*, 557(1), 99–108. DOI: [10.1016/j.mrgentox.2003.10.004](https://doi.org/10.1016/j.mrgentox.2003.10.004)
- Yin, S., Tang, M., Chen, F., Li, T. & Liu, W. (2017). Environmental exposure to polycyclic aromatic hydrocarbons (PAHs): The correlation with and impact on reproductive hormones in umbilical cord serum *. *Environmental Pollution*, 220, 1429–1437. DOI: [10.1016/j.envpol.2016.10.090](https://doi.org/10.1016/j.envpol.2016.10.090)
- Zhang, Y., Dong, S., Wang, H., Tao, S. & Kiyama, R. (2016). Biological impact of environmental polycyclic aromatic hydrocarbons (ePAHs) as endocrine disruptors *. *Environmental Pollution*, 213(November), 809–824. DOI: [10.1016/j.envpol.2016.03.050](https://doi.org/10.1016/j.envpol.2016.03.050)